

DEUTSCHES ELEKTRONEN-SYNCHROTRON DESY

DESY 76/40
August 1976



Measurement of the Branching Ratios for the Decays

$$J/\psi \rightarrow \rho\pi \text{ and } J/\psi \rightarrow \gamma\eta'$$

by

W. Bartel, P. Duinker, J. Olsson, P. Steffen

Deutsches Elektronen-Synchrotron DESY, Hamburg

J. Heintzelman, G. Hertzmann, R. D. Stoenes, S. Strubbeke, F. Ruestefeld

B. Schmeier, A. Wagner, A. W. Wenzel

Abstract:

Decays of the $J/\psi(3.1)$ resonance into final states with two charged hadrons and two photons are investigated. Branching ratios for the decays $J/\psi \rightarrow \rho\pi$ and $J/\psi \rightarrow \gamma\eta'$ are determined to be

$$\frac{\Gamma(J/\psi \rightarrow \rho\pi)}{\Gamma(J/\psi \rightarrow \text{all})} = (1.0 \pm 0.2) \cdot 10^{-2}$$

$$\frac{\Gamma(J/\psi \rightarrow \gamma\eta')}{\Gamma(J/\psi \rightarrow \text{all})} = (2.4 \pm 0.7) \cdot 10^{-3}$$

Upper limits for the same decay modes of $\psi'(3.7)$ are also determined.

2 HAMBURG 52 · NOTKESTIEG 1

To be sure that your preprints are promptly included in the
HIGH ENERGY PHYSICS INDEX ,
send them to the following address (if possible by air mail) :

DESY
Bibliothek
2 Hamburg 52
Notkestr. 1
Germany

Measurement of the Branching Ratios for the Decays
 $J/\psi \rightarrow \rho\pi$ and $J/\psi \rightarrow \gamma\eta'$

W. Bartel, P. Duinker, J. Olsson, P. Steffen
Deutsches Elektronen-Synchrotron DESY, Hamburg

J. Heintze, G. Heinzelmann, R.D. Heuer, R. Mundhenke, H. Rieseberg,
§ B. Schürlein[†], A. Wagner, A.H. Walenta
Physikalisches Institut der Universität Heidelberg

Abstract

Decays of the $J/\psi(3.1)$ resonance into final states with two charged hadrons and two photons are investigated. Branching ratios for the decays $J/\psi \rightarrow \rho\pi$ and $J/\psi \rightarrow \gamma\eta'$ are determined to be

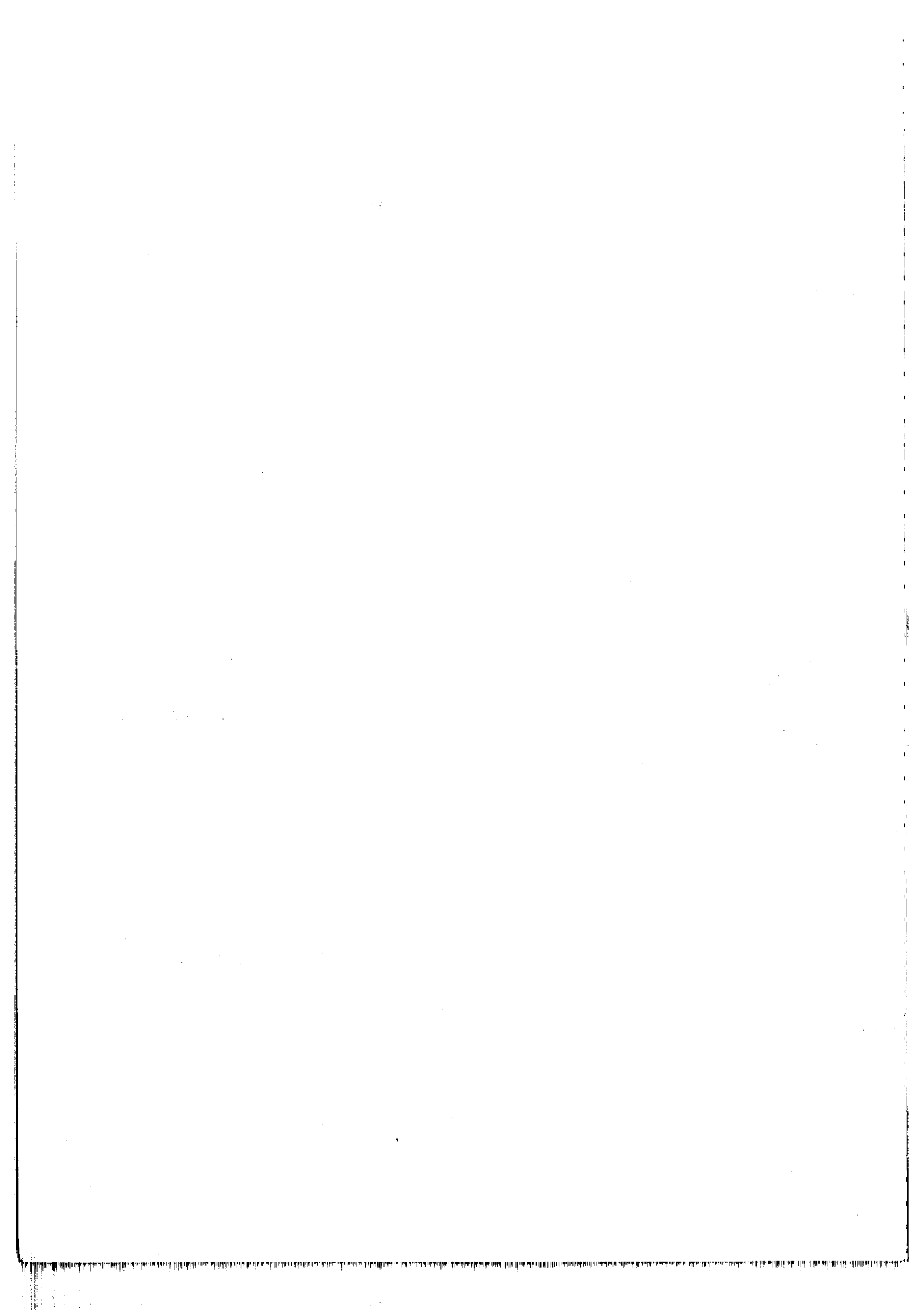
$$\frac{\Gamma(J/\psi \rightarrow \rho\pi)}{\Gamma(J/\psi \rightarrow \text{all})} = (1.0 \pm 0.2) \cdot 10^{-2}$$

$$\frac{\Gamma(J/\psi \rightarrow \gamma\eta')}{\Gamma(J/\psi \rightarrow \text{all})} = (2.4 \pm 0.7) \cdot 10^{-3}$$

Upper limits for the same decay modes of $\psi'(3.7)$ are also determined.

§ Now at IDAS GmbH, Limburg

† Present address: BNL, Upton, New York



We report in this letter on a measurement of the branching ratios for the decays

$$J/\psi \rightarrow \rho\pi \quad (1)$$

$$J/\psi \rightarrow \gamma\eta' \quad (2)$$

and



Both decays result in a final state consisting of two charged particles and two photons. While the decay (1) can be studied with missing mass techniques based upon the detection of charged particles alone^{1,2}, the analysis of (2) requires in addition the detection of γ -rays. The experiment presented here was done with a non-magnetic detector, which gives the directions of the two charged particles and of the two photons in the final state. The data were taken at the DESY storage rings DORIS.

Experimental set-up

The detector is shown in fig. 1. It consists of:

- a) an internal cylindrical detector to measure directions of charged particles and photons,

- b) an arrangement of NaI and lead glass counters to measure the energies of electrons and photons as well as the energy losses of hadrons and muons,

- c) a hadron absorber to identify muons.

The internal detector (CD in fig. 1) consists of three cylindrical double drift chambers³, two scintillation counter hodoscopes (H and H') and a removable photon converter. The arrangement encloses the full range of the azimuthal angle ϕ and the interval 30° to 150° for the polar angle θ thus subtending 86 % of the full solid angle. The region of small angle scattering ($15^\circ < \theta < 30^\circ$ and $150^\circ < \theta < 165^\circ$) is covered by two additional scintillation counter hodoscopes (M) of 16 elements each. With these counters the solid angle for detection of charged particles is extended to 95 % of 4π .

Each double drift chamber has 128 anode wires to measure the ϕ coordinates and 80 cathode strips to measure the θ coordinates. The $\phi-\theta$ correlation in multi-track events is achieved by comparing the drift times on the anode wires with the timings of the induced signals on the cathode strips. The accuracy obtained for the angle measurements of charged tracks is $\delta\phi = 4$ mrad and $\delta\theta = 30$ mrad (FWHM).

Each element of the scintillation counter hodoscopes H and H' covers the angular intervals of $\Delta\phi = 22.5^\circ$, $30^\circ < \theta < 90^\circ$ or $90^\circ < \theta < 150^\circ$. Various track multiplicities can be selected for triggering purposes by coincidences between corresponding cells of H and H'.

The removable photon converter consists of mercury contained in an epoxy fibre glass vessel shaped such that all photons originating from the centre see a converter thickness of two radiation lengths. The coordinates of conversion points are measured in the last drift chamber with accuracies of $\delta\phi = 75$ mrad and $\delta\theta = 65$ mrad (FWHM).

A NaI and lead glass counter arrangement surrounds the cylindrical detector. On each side there are 12 NaI and 20 lead glass blocks with a total thickness of 13 radiation lengths. The energy resolution for electrons and photons is 11 % at 0.03 GeV, 18 % at 0.2 GeV and 11 % at 1.0 GeV (FWHM). In the presence of the mercury converter the resolution is degraded. The top and bottom parts of the inner detector are covered by lead glass bars, 18 cm = 8 radiation lengths thick and 140 cm long. Phototubes are attached to both ends to compensate for light attenuation. The energy resolution is 30 % at 1.0 GeV.

For unconverted photons, the directions can be determined from the ratios of pulse heights in adjacent blocks and from time difference measurements in the lead glass bars. The accuracies (FWHM) are $\delta\theta = 100$ mrad and $\delta\phi = 240$ mrad (side walls) and $\delta\theta = 240$ mrad and $\delta\phi = 150$ mrad (top and bottom).

Muons with a momentum above 1.0 GeV/c penetrate the hadron absorber, which consists of 60 cm thick iron plates, in addition to the NaI/lead glass counter blocks. The muons are detected in drift chambers covering a solid angle of 45 % of 4π .

Cosmic rays can be identified by a time of flight measurement between the scintillation counters C. The scintillation counters R around the beam pipe are used to veto background triggers from the beam halo.

The trigger consists of several combinations of a minimum track multiplicity with a minimum energy E observed in the NaI/lead glass counters, as follows:

≥ 3 tracks	and	$E \geq .3$ GeV
≥ 2 tracks	and	$E \geq .4$ GeV
≥ 1 track	and	$E \geq .9$ GeV
≥ 0 track	and	$E \geq 1.5$ GeV

A minimum ionizing particle traversing the NaI/lead glass blocks leads to an average observed energy of .22 GeV. The zero prong trigger requires in addition to the minimum energy of 1.5 GeV at least one hadoscope counter H to be hit, indicating the conversion of a γ ray.

Data analysis

In the present study, only data taken with the mercury converter in place are used. In these data we find after background subtraction 662000 hadronic J/ψ decays. Including corrections for acceptance losses (~5 %), pattern recognition losses (~7 %) and J/ψ decays into two charged particles (~14 %, e^+e^- , $\mu^+\mu^-$, $p\bar{p}$), 871000 J/ψ decays are obtained. This number is used as a normalisation. It does not include a small fraction of events with only neutral particles in the final state (~1 %, these events will be treated in a subsequent paper). The error on the normalisation is 7 %, mainly due to systematic uncertainties.

In order to select candidates for reactions (1) and (2), events with two converted photons and two tracks originating from the interaction region are selected. The sample thus defined consists of 3299 events. The momenta of the final state particles are kinematically reconstructed using their measured directions in space and assuming the charged particles to be pions. 60 % of the events lead to solutions with negative energies, because of additional particles or photons escaping detection or because of errors in the coordinate measurements of the photons (36 % and 24 %, respectively). 1265 events give solutions with positive energies and are accepted. A comparison between the γ -ray energies measured in the apparatus and the corresponding fitted energies removes 106 events. The final sample then consists of 1159 events.

In a scan of a subsample, the background contamination was determined to be 8 ± 2 %. This background consists of events with misidentified topologies (e. g. 2 prong, 3 γ events) and of real 2 prong, 2 γ events with wrongly assigned coordinates. The effective mass distributions of this background are flat and therefore no significant contribution to the reactions (1) and (2) is expected from these events.

Analysis of the decay $J/\psi \rightarrow \rho\pi$
 In all 3 charge modes ($\rho^+ \pi^-$, $\rho^- \pi^+$ and $\rho^0 \pi^0$) with the subsequent decay $\rho \rightarrow \pi\pi$, the final state consists out of $\pi^+ \pi^- \gamma\gamma$. Invariant mass distributions for the $\gamma\gamma$, $\pi^+ \pi^-$ and $\pi^0 \gamma\gamma$ systems are shown in Fig. 2a-c. Clear signals of π^0 and of neutral and charged ρ are seen. The hatched histograms of fig. 2b and 2c are obtained by restricting the invariant mass $m_{\gamma\gamma}$ to the π^0 interval ($0 < m_{\gamma\gamma} < .35$ GeV). The Dalitz plot for the 613 events fulfilling this condition is shown in Fig. 3.

A background contribution to the charged ρ signal of fig. 2c is due to the decay $J/\psi \rightarrow K^+ K^{*+}(892)$, $K^{*+} \rightarrow K^+ \pi^0$, since the assignment of the pion mass to the kaons shifts the $K^{*+}(892)$ mass to 720 MeV. From the measured branching ratio for this decay^{4,¶}, a contribution of 44 ± 11 events to the ρ peak is expected. The number of events due to reaction (1) is calculated by fitting a relativistic Breit-Wigner curve folded with a Gaussian resolution function and a 2nd order polynomial background. These fits are shown as full curves in fig. 2b and 2c, together with the fitted background. A total of 203 ± 34 events are obtained in the $\rho^0 \pi^0$ channel while 340 ± 100 are assigned to the charged ρ decays (after subtraction of the $K^{*+}(892)$ contribution). The overall efficiencies are calculated using Monte Carlo methods, assuming a $1 + \cos^2\theta$ decay angular distribution ($\theta =$ angle between beam and ρ). They are found to be 5.9 ± 0.5 % and 6.2 ± 0.5 % for $J/\psi \rightarrow \rho^0 \pi^0$ and $J/\psi \rightarrow \rho^\pm \pi^\mp$, respectively.

Normalizing to the total number of J/ψ decays a branching ratio of

$$\frac{\Gamma(J/\psi \rightarrow \rho\pi)}{\Gamma(J/\psi \rightarrow \text{all})} = (1.0 \pm 0.2) \cdot 10^{-2}$$

is obtained. It agrees well with other experiments^{1,2}. The ratio

$$\frac{\Gamma(J/\psi \rightarrow \rho^0 \pi^0)}{\Gamma(J/\psi \rightarrow \rho^\pm \pi^\mp)} = 0.63 \pm 0.22$$

is in good agreement with the value 0.5, expected for an isospin assignment of $I = 0$ for the J/ψ particle¹.

[¶] If the branching ratio given in ref. 2 is used, the $K^{*+}(892)$ contribution to the ρ^\pm peak is higher (82 ± 25 events).

Analysis of the decay $J/\psi \rightarrow \gamma\eta'$

The decay chain $J/\psi \rightarrow \gamma\eta'$, $\eta' \rightarrow \gamma\rho$, $\rho \rightarrow \pi^+\pi^-$ leads to final states with two charged pions and two photons. This type of events is therefore included in the sample of 1159 events defined above.

The invariant mass distribution of the $\pi^+\pi^-$ system is shown in fig. 2d. An η' signal is clearly visible. The signal becomes more prominent when the $m_{\pi^+\pi^-}$ invariant mass is confined to the ρ band ($0.55 < m_{\pi^+\pi^-} < 1.0$ GeV) and when events with the η^0 mass in the η^0 band are excluded (hatched histogram of fig. 2d). Since every event enters twice into the plot, a reflection of the η' signal is observed in the high mass region which compares well with a Monte Carlo simulation shown as the dashed curve in fig. 2d.

The absolute number of events due to reaction (2) is obtained by fitting a gaussian resolution function to the experimental invariant mass distribution of fig. 2d assuming a constant background. The mass resolution is found to be $\sigma = 40 \pm 9$ MeV and a total of 57 ± 13 events are assigned to the decay (2). The efficiency is calculated in the same way as for reaction (1) and is determined to be 9.1 ± 0.7 %. A branching ratio of

$$\frac{\Gamma(J/\psi \rightarrow \gamma\eta')}{\Gamma(J/\psi \rightarrow \text{all})} = (2.4 \pm 0.7) \cdot 10^{-3}$$

is obtained, which is well below the upper limit of 1.7 % given in ref. 5. The error contains the statistical error as well as the error of the decay width of $\eta' \rightarrow \rho\gamma$ ⁶⁾ and a 5 % systematic error.

The ratio $\Gamma(J/\psi \rightarrow \eta\eta')/\Gamma(J/\psi \rightarrow \eta\eta)$ will be discussed in connection with a measurement of $\Gamma(J/\psi \rightarrow \eta\eta)$ in a subsequent paper.

The decays $\psi' \rightarrow \rho\pi$ and $\psi' \rightarrow \eta\eta'$

In a sample of 191000 ψ' -decays we have searched for the corresponding reactions $\psi' \rightarrow \rho\pi$ and $\psi' \rightarrow \eta\eta'$, $\eta' \rightarrow \gamma\rho^0$, in the same way as described above. No signal is seen for either decay, leading to the following upper limits (90 % C.L.) for the branching ratios:

$$\frac{\Gamma(\psi' \rightarrow \eta\eta')}{\Gamma(\psi' \rightarrow \text{all})} < 1.1 \cdot 10^{-3}$$

and

$$\frac{\Gamma(\psi' \rightarrow \rho\pi)}{\Gamma(\psi' \rightarrow \text{all})} < 1.0 \cdot 10^{-3}.$$

Acknowledgment

It is a pleasure to acknowledge the excellent and efficient work of the DORIS machine group, of the DESY Hallendienst and of the Heidelberg University workshops. We thank K. Bruder, H. Matsumura, H.J. Seidel and J. Zimmer for their competent technical assistance and for their help in running the experiment. Furthermore, the members of the Heidelberg group thank the DESY directorate for their kind hospitality.

This work was partly supported by the Bundesministerium für Forschung und Technologie.

References

1. B. Jean-Marie et al., PRL 36 (1976) 291.
2. W. Braunschweig et al., DESY 76/28 (1976).
3. J. Heintze, A.H. Walenta, Nucl. Instr. and Meth. 111 (1973) 461;
A.H. Walenta, IERC Transactions on Nuclear Science 22 (1975) 251;
A.H. Walenta, RHEI/M/H21 (1972) 116.
4. F. Vanucci et al., SLAC-PUB-1724
5. R. Baldini-Celio et al., PL 58B (1975) 475.
6. Review of Particle Properties, Rev. Mod. Phys. 48, 2, II, (1976)

Figure Captions

- Fig. 1 Apparatus of DESY-Heidelberg Collaboration.
Top: side view along the beam, bottom: view from above.
- Fig. 2 Invariant mass distributions of 2- and 3-particle combinations.
- Fig. 3 Dalitz plot for events with $(0. < m_{\gamma\gamma} < .35 \text{ GeV})$.
- The curves are described in the text.
- Fig. 1 Apparatus of DESY-Heidelberg Collaboration.
Top: side view along the beam, bottom: view from above.
- Fig. 2 Invariant mass distributions of 2- and 3-particle combinations.
- Fig. 3 Dalitz plot for events with $(0. < m_{\gamma\gamma} < .35 \text{ GeV})$.
- The curves are described in the text.
- Fig. 2 Invariant mass distributions of 2- and 3-particle combinations.
- a) $M(\gamma\gamma)$.
b) $M(\pi^+\pi^-)$. Hatched histogram: events with $(0. < m_{\pi^+\pi^-} < .35 \text{ GeV})$.
c) $M(\pi^+\gamma\gamma)$, 2 entries/event. Hatched histogram as in fig. 2b.
d) $M(\pi^+\pi^-\gamma)$, 2 entries/event. Hatched histogram: events with
 $(m_{\pi^+\pi^-} > .35 \text{ GeV})$ and $(.55 < m_{\pi^+\pi^-} < 1.00 \text{ GeV})$.

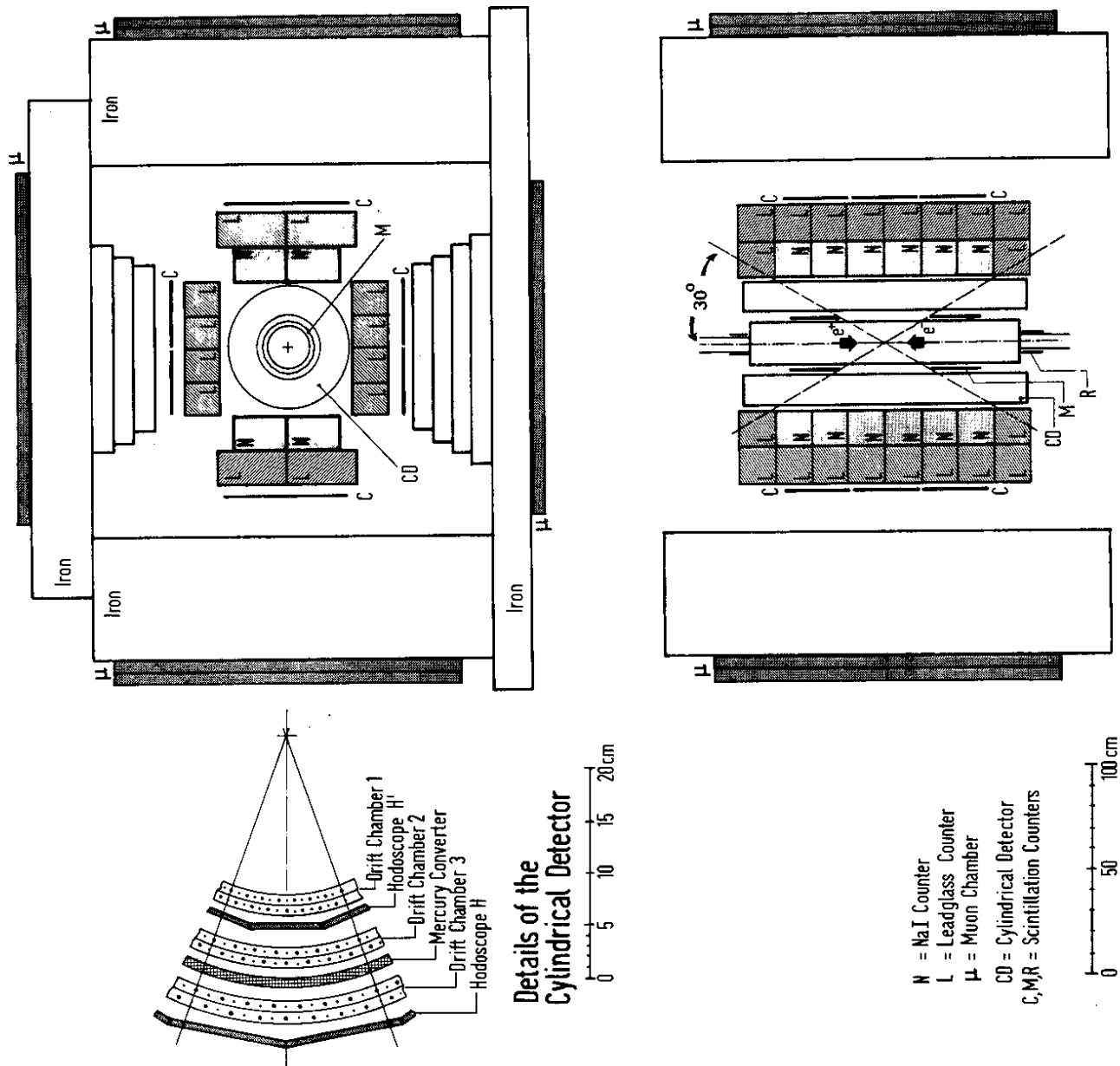


Figure 1

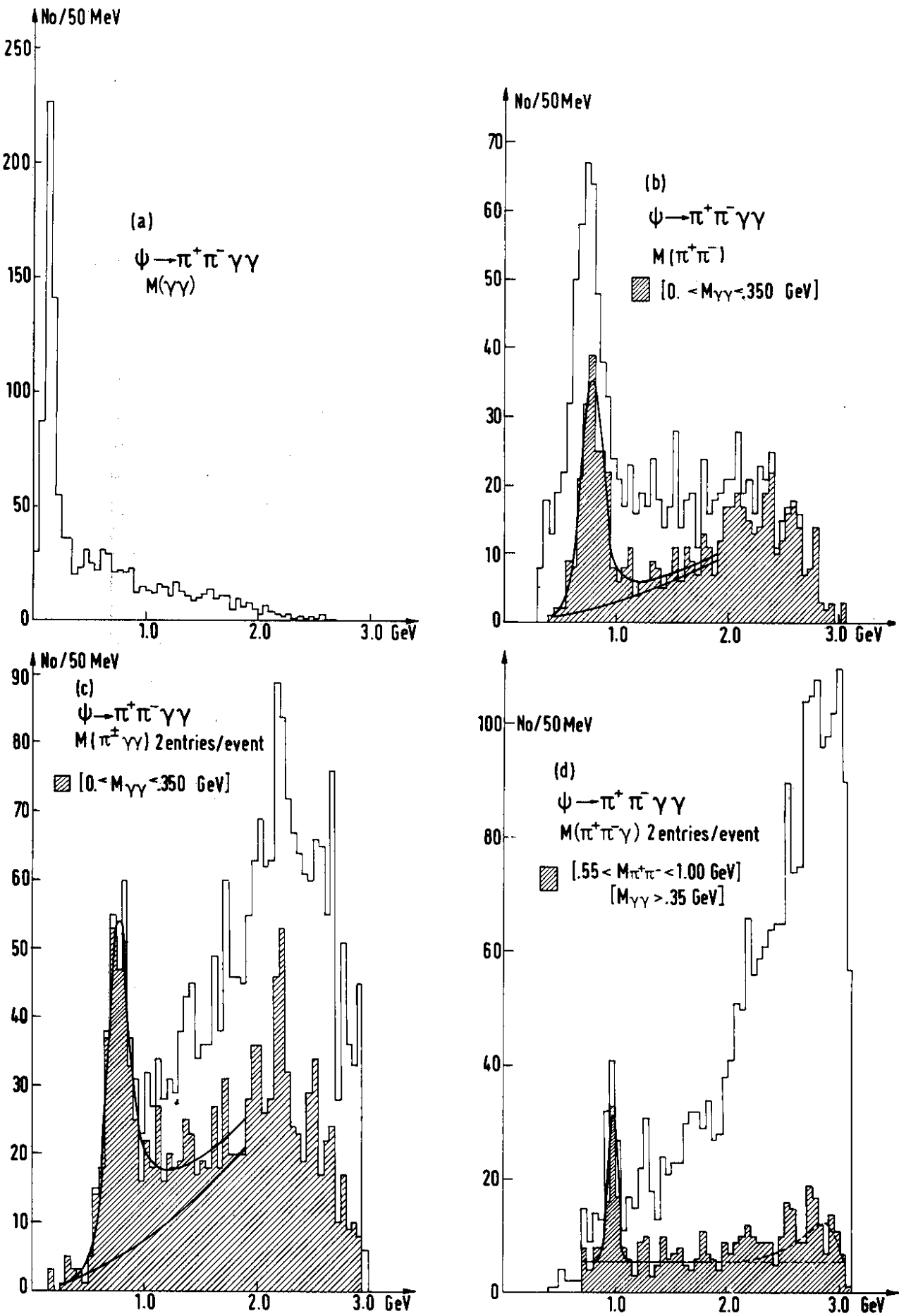


Figure 2

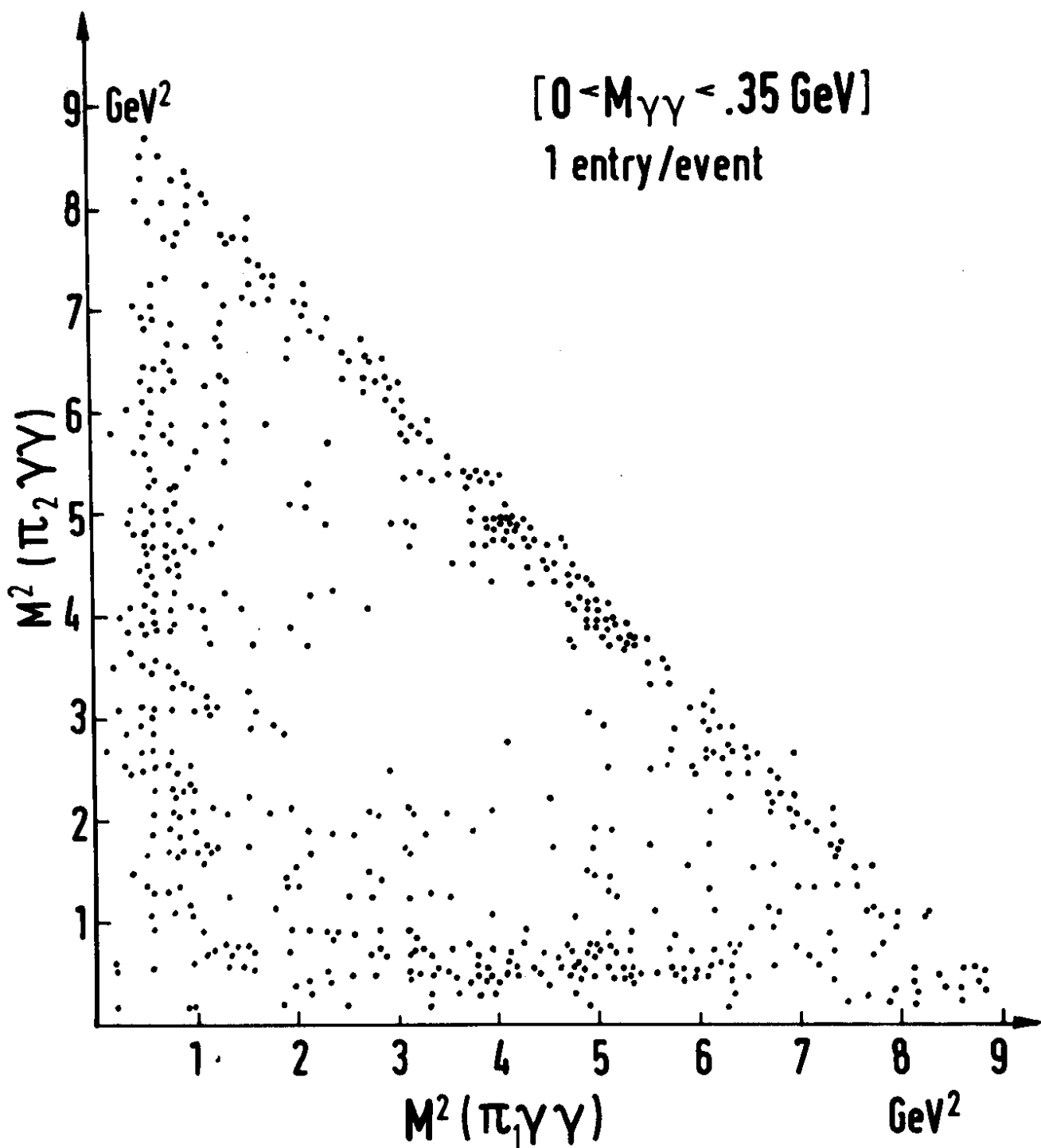


Figure 3

